

AGB variables in Baade’s windows

M. Schultheis¹, I.S. Glass²

¹*Institut d’Astrophysique, 98 bis Blvd Arago, F75014 Paris, France (email: schulthe@iap.fr)*

²*South African Astronomical Observatory, PO Box 9, Observatory 7935, South Africa (email: isg@sao.ac.za)*

Received 2000

ABSTRACT

In this work, a sample of luminous M-type giants in the Baade’s Windows towards the inner Galactic Bulge is investigated in the near-infrared. The ISOGAL survey at 7 and 15 μm has given information concerning the mass-loss rates of these stars and their variability characteristics have been extracted from the MACHO database. Most are known to be semi-regular variables (SRVs). Here we discuss how their IJK_S -region colours depend on period and the presence or absence of mass-loss, using results mainly taken from the DENIS and 2MASS surveys.

In order to compare their colours with solar neighbourhood stars, photometric colours on the DENIS, 2MASS and ESO photometric systems have been synthesized for objects in the spectrophotometric atlas of Lançon and Wood (2000). In addition, they have been used to predict the differences in colour indices when stars with strong molecular bands are observed using different photometric systems.

The SRVs are found to inhabit the upper end of the $J - K_S$, K_S colour-magnitude diagram, lying just below the Miras. High mass-loss rates are associated with high luminosity. The near-infrared colours of the semi-regular variables increase in a general way with period and are reddest for the stars with significant mass-loss. The average colours of Mira variables, whose periods start at around 200 days in the Bulge, are bluer than those of the semi-regulars at this period, particularly in $J - H$, thanks to the association of deep water-vapour bands with large amplitude.

Key words: Galaxy: center, stars: variables: others, stars: AGB and post-AGB, surveys

1 INTRODUCTION

The ISOGAL programme (Omont et al. 1999, 2001) has made use of the ISO satellite to obtain detailed surveys of sample areas of the inner Bulge and the Galactic Plane at two mid-infrared wavelengths, 7 μm and 15 μm , with the intention of investigating the longitude and latitude variations of stellar properties and their bearing on galactic structure. Because many of the fields are highly obscured, parts of the relatively clear Baade’s Windows were included for comparison purposes (Glass et al. 1999). By studying the contents of the latter at infrared and visible wavelengths one obtains a picture of the basic stellar population in the Bulge, to which more heavily obscured fields, observable only in the infrared, can be compared. Fields of 15×15 arcmin² from each of Sgr I and NGC 6522 were thus included in the ISOGAL work. These were centred at $\ell = +1.37^\circ$, $b = -2.63^\circ$ and $\ell = +1.03^\circ$, $b = -3.83^\circ$ respectively.

Near-infrared data at $I(0.79 \mu\text{m})$, $J(1.22 \mu\text{m})$ and $K_S(2.14 \mu\text{m})$, where the subscript S denotes ‘short’, for both windows are now available from the DENIS survey (Epchtein, 1998) and for the Sgr I window only at

$J(\sim 1.22 \mu\text{m})$, $H(1.65 \mu\text{m})$ and $K_S(2.16 \mu\text{m})$ from 2MASS (Skrutskie, 1998). In addition, photometry on the Caltech-CTIO system by Frogel and Whitford (1987, hereafter FW) was obtained for many of the M stars in the objective prism survey of the NGC 6522 field by Blanco, McCarthy and Blanco (1984) and Blanco (1986). A comparison of stars detected by ISOGAL with the latter survey indicates that, except for a few probable foreground stars, none with spectral type earlier than M2 were seen. The rate of detection increased with sub-type, reaching 100% at M6.

Several previous surveys of these fields for variable stars have been made. I -band photography by Lloyd Evans (1976) yielded identifications and periods of many Miras. A search for the near-infrared counterparts of IRAS sources (Glass 1986) revealed some additional long-period, large-amplitude variables that were not found in the I -band survey. Infrared observations of nearly all the long-period, large-amplitude variables in Sgr I were obtained by Glass et al. (1995), so that the sample is probably complete and the period distribution, period-luminosity relation and period-colour properties of Miras in Sgr I may be regarded as known.

The Sgr I and NGC 6522 windows formed part of the

Table 1. Filter transmission data

DENIS		
Band	cut-on (μm)	cut-off (μm)
<i>I</i>	0.73	0.87
<i>J</i>	1.10	1.39
<i>K_S</i>	1.98	2.31
2MASS		
Band	cut-on (μm)	cut-off (μm)
<i>J</i>	1.11	1.36
<i>H</i>	1.50	1.80
<i>K_S</i>	2.00	2.32

Notes:

The cut-on and cut off wavelengths are taken to be the 50% transmission values.

The DENIS transmissions include effects due to the earth's atmosphere. The effective long wavelength end of the *J*-band is determined by atmospheric transmission at about $1.35\mu\text{m}$.

MACHO gravitational lens survey. Alard et al. (2001) present variability information for all 332 stars that have been detected at both ISOGAL and both MACHO wavelengths: *v* ($\sim 0.54\mu\text{m}$), *r* ($\sim 0.70\mu\text{m}$), $7\mu\text{m}$ and $15\mu\text{m}$. Nearly all of the 332 objects were found to be semi-regular variables (SRVs) with periods of from 10 to 230 days and amplitudes < 1 mag. and will be referred to collectively here as the ISOGAL/MACHO sample. The SRVs in the present fields outnumber the Miras by a factor of about 20. Note that the area surveyed by MACHO omits about 10% of each ISOGAL field.

We have assumed that the interstellar absorption is $A_V=1.5$ mag for both fields. We take in addition $A_I=0.59A_V$, $A_J=0.245A_V$, $A_H=0.142A_V$ and $A_K=0.085A_V$, based on the van de Hulst curve (Glass, 1999).

2 COMPARISON OF DENIS, 2MASS AND OTHER PHOTOMETRY

All objects falling in the ISOGAL fields have been extracted from the DENIS and 2MASS databases as well as the FW work. A search radius of $2''$ was chosen to avoid mis-identifications. The DENIS observations form part of a dedicated survey of the Galactic Bulge (Simon et al., in preparation). The 2MASS observations are limited to Sgr I and a small part of NGC 6522 with the consequence that only 225 of the 332 ISOGAL/MACHO stars fall within the common area. In this and the following section we show by direct comparisons that the available information is consistent.

Firstly, it is necessary to consider what effect the different filter systems may be expected to have on the photometry. The DENIS filters have been convolved with the typical atmospheric transmission at La Silla (Fouqué et al. 2000), where the survey was made. A summary of the available data is given in table 1. For details of the filter transmissions and systematic response curves, see Fouqué et al (2000) for DENIS; 2MASS web pages for 2MASS.

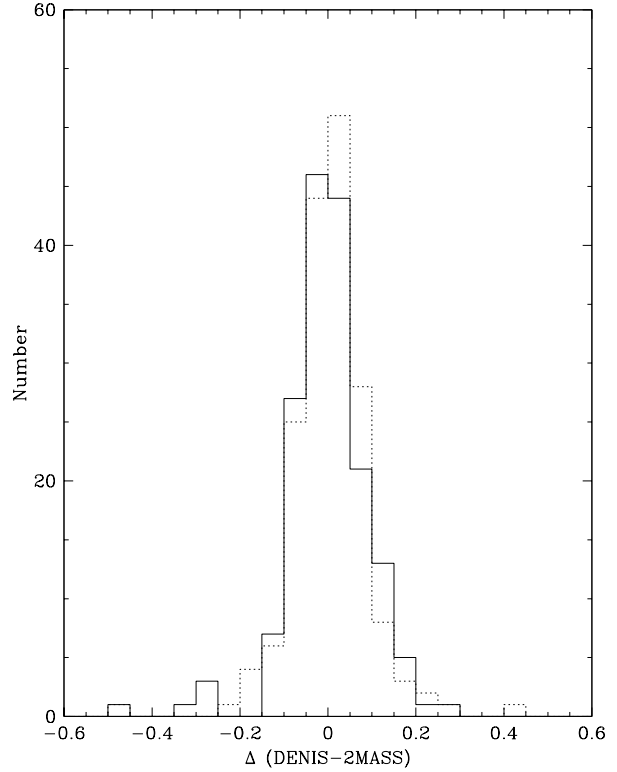


Figure 1. Histograms of differences between DENIS and 2MASS *J* and *K_S* data for ISOGAL/MACHO variables identified in both data sets. The solid line is *J* and the dotted line is *K_S*.

2.1 Photometric passbands

Important differences between systems occur in the *J*- and *K*-bands. The Caltech-CTIO system as used by FW has an effective *J* wavelength (see J_{old} in fig. 4 of Persson et al. 1998) of about $1.25\mu\text{m}$, considerably longer than that of DENIS ($\sim 1.22\mu\text{m}$).

The *H* and *K* bands of the SAAO photometric system are very close to those of the ESO system (see Bouchet, Schmider & Manfroid, 1991). The SAAO Mira data for the Baade's Window field (Glass et al. 1995), to which we refer later on, were taken with the MkIII photometer, whose effective wavelength at *J* is $\sim 1.22\mu\text{m}$ (Glass, 1993). This is essentially identical to J_{DENIS} .

Fig 1 shows histograms of differences between DENIS and 2MASS *J* and *K_S* data for MACHO variables identified in both data sets. It is seen that the agreement is satisfactory, both ΔJ and ΔK_S being less than 0.01 mag on average, with $\sigma \sim 0.12$ and 0.09 for the two bands respectively. The two surveys were conducted during the same year and season. We have also plotted the differences between the DENIS and 2MASS photometry for all stars in common in the ISOGAL field against (*J*-*K*) and find no significant trend.

Fig 2 shows histograms of the differences between the DENIS and the FW data for NGC 6522 in the sense (DENIS – FW). It should be noted that the size of the sample is small and some degree of variability is likely in almost all the stars. The FW *I*-band data are from the photographic survey by Blanco et al. (1984) and Blanco (1986). As might

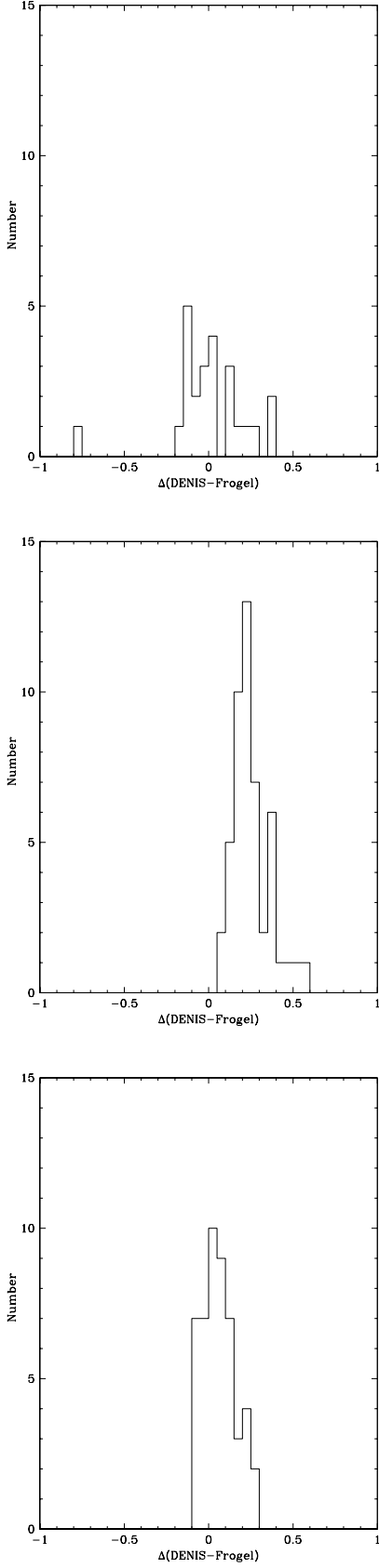


Figure 2. Histograms of differences between DENIS and FW data for ISOGAL/MACHO objects in common in NGC 6522. The left histogram represents the I data; $\langle \Delta I \rangle = -0.002$, s.d. = 0.4. The centre histogram represents the J data; $\langle \Delta J \rangle = 0.24$ s.d. 0.12. The right histogram represents K ; $\langle \Delta K \rangle = 0.04$ s.d. 0.11.

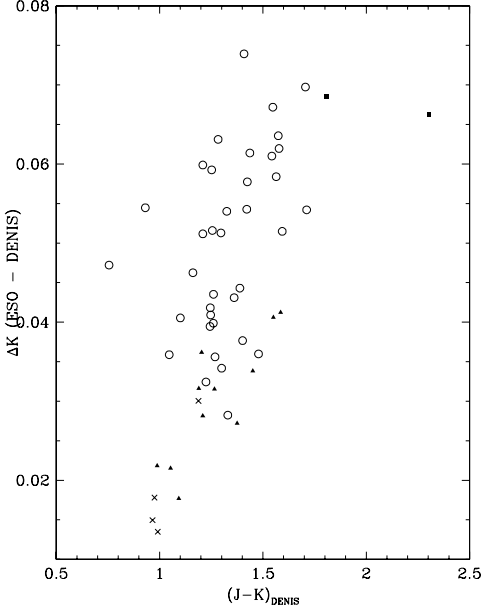


Figure 3. Differences between ESO standard K magnitudes and DENIS K_S obtained by synthetic photometry, based on spectrophotometry by LW, for Giants (crosses), SRVs (triangles), field Miras (open circles) and Bulge Miras (solid squares).

be expected, ΔI shows a large scatter (0.4 mag) but its average value is almost zero (note that the number of objects compared is small).

ΔJ shows an average of 0.24 mag with $\sigma = 0.12$. According to the conventional transformation between the Caltech and SAAO (and similar) systems, defined by observations of standard stars in common, part at least of the difference (~ 0.14 mag) can be attributed to the effective wavelengths of the filters. There is evidence that transformation of the J mags of late-type variables requires a stronger colour term than the standard stars (Glass 1993).

ΔK is 0.04 with $\sigma = 0.11$. Differences arise from the shorter cut-on and cut-off wavelengths of the K_S filter relative to K . These will have strong effects if the spectra show well-developed H_2O or CO bands as is the case for Mira variables and other very late-type M stars. K_S will include more of the water-vapour band and less of the CO first overtone band than K .

We have constructed synthetic K_{ESO} and K_{DENIS} data from the Lançon & Wood (2000, hereafter LW) spectrophotometry (see also section 5). In this exercise the spectral energy distributions were convolved with the DENIS filter profiles and the estimated average atmospheric transmission at La Silla. The zero-points of the synthetic photometry were obtained from spectrophotometry of Vega, which was taken to have magnitude 0.0 at all wavelengths. We found that most categories of late-type stars show $\Delta(K - K_{\text{DENIS}}) \sim 0.03$ mag with s.d. ± 0.01 mag. However, the difference increases to 0.05 with p-p scatter ± 0.025 for field Miras (see fig. 3). Two long-period Bulge Miras in the LW sample show $\Delta(K - K_{\text{DENIS}}) \sim 0.07$ mag.

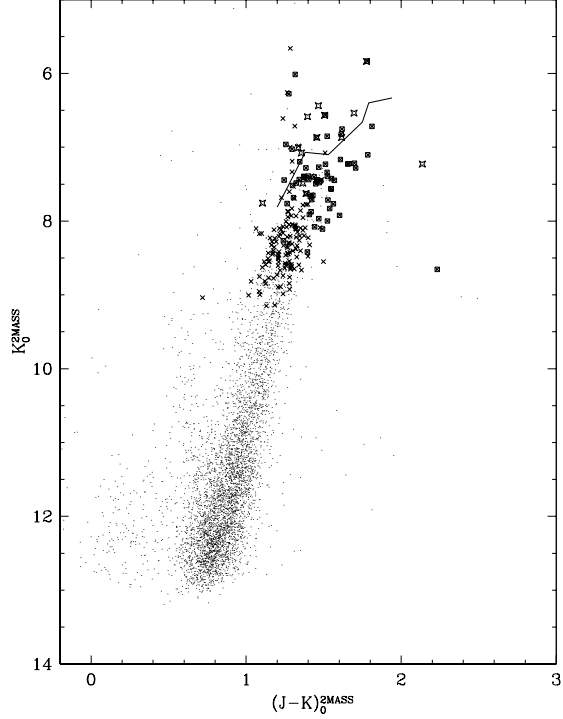


Figure 5. $K_{S,0}, (J - K_S)_0$ diagram from 2MASS data. The small dots are stars from the general field of Sgr I. Crosses represent ISOGAL/MACHO SRVs with low mass-loss; squares those with high. Miras in the ISOGAL/MACHO field are shown with starred symbols. The segmented line shows magnitudes and colours averaged by period groups from Glass et al. (1995). The Miras are overlapped by the more luminous SRVs. Note that, for M stars, K is approximately related to m_{bol} by $m_{\text{bol}} \sim K + 3$. See text concerning the isolated ISOGAL/MACHO star at $(K_{S,0}, (J - K_S)_0) = (8.65, 2.23)$.

3 STAR COUNTS AND COMPLETENESS

Fig 4 shows histograms of near-infrared photometry of objects from DENIS and 2MASS in the Sgr I Baade's window and may be used to examine the completeness of these surveys as functions of magnitudes in the J and K_S bands. The area considered is slightly less than the total ISOGAL field in order to avoid edge effects.

At J it is evident that there are slightly fewer 2MASS sources than DENIS in most magnitude bins. The two histograms deviate systematically for $J > 13.0$ and indicate that DENIS is probably complete to about 13.5 ($\sim 80\%$ of the maximum of the histogram).

In K_S it is once again evident that the 2MASS detections are slightly fewer than the DENIS to about 12.0. The limit of 2MASS appears to be about 0.2 mag fainter than DENIS.

DENIS I appears complete to about mag 15.0 while 2MASS H is complete to about 12.5.

For both 2MASS and DENIS the sensitivity is mostly limited by confusion in the J , H and K_S bands. The densities of sources detected in DENIS reach 73 pixels/object at I , 6 pixels/object at J and 15 pixels/object at K_S . The corresponding figures for 2MASS are 13 pixels/object in J

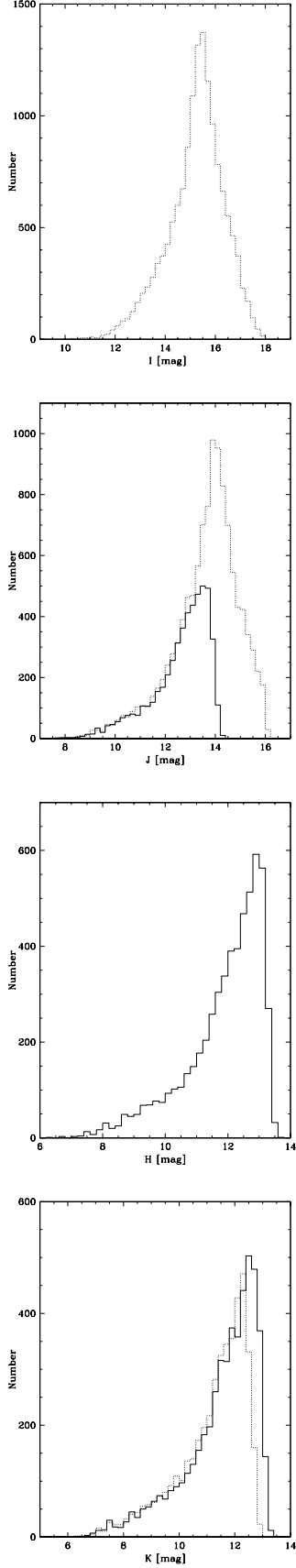


Figure 4. Histograms of near-infrared photometry of objects from the DENIS and 2MASS surveys in SgrI. From left to right: I , J , H and K_S . In the J and K_S diagrams, the DENIS histograms are shown dotted and the 2MASS solid.

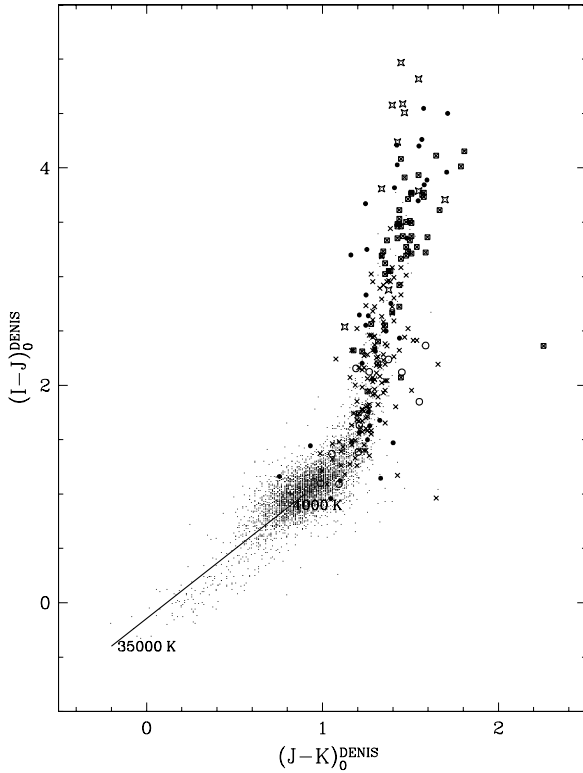


Figure 6. $(I - J)_0$ vs $(J - K)_0$ for ISOGAL/MACHO from DENIS. Crosses represent ISOGAL/MACHO SRVs with low mass-loss; squares those with high. Small points represent the remainder of the DENIS detections in the Sgr I field. The line shows the location of earlier-type giants from Pickles (1998). Open circles are synthetic colours of SRVs and closed circles of Miras derived from the LW spectrophotometry.

and K_S and 12 pixels/object in H . Almost certainly, the reliability of detection and the accuracy of the photometry decreases towards the faint end, but a full discussion of these issues awaits the publication of the catalogues.

There are 201 ISOGAL/MACHO stars in Sgr I, of which 196 were detected by DENIS and 187 (of which 185 were in common with DENIS) by 2MASS. The two 2MASS stars not detected by DENIS lay along the edge of the field and may have been lost due to slightly different astrometric solutions.

4 COLOUR-MAGNITUDE DIAGRAM

Fig 5 shows the $K_{S,0}, (J - K_S)_0$ diagram for the 2MASS data from Sgr I. Although the 2MASS data show smaller scatter, the DENIS data show fewer objects with outlying high $(J - K_S)_0$ colours. An investigation of such objects from the general field of Sgr I showed that in DENIS some were not recorded, some had J but not K detections and the remainder had ordinary $J - K$ colours.

We distinguish with special symbols the ISOGAL/MACHO variables with high mass-loss, defined by $[7] - [15] > 0.6$ and $[15] < 7.5$, the latter criterion being used to eliminate objects with high probable errors. The diagram is dominated by the sequence of late-type giants having the

ISOGAL/MACHO objects towards the tip. The SRVs with infrared excesses are generally redder and more luminous than the others. The Miras lie at or near the tip and are overlapped by the SRVs. Some apparently luminous stars in this diagram may lie in the foreground.

There is also a vertical sequence of objects at $(J - K_S)_0 \sim 0.6$ which may represent foreground stars.

The isolated star at $(K_{S,0}, (J - K_S)_0) = (8.65, 2.23)$ is the reddest object in Fig 9 (the $[15]$ vs $[7] - [15]$ diagram) of Glass et al (1999). Because of doubt about its (preliminary) ISOGAL photometry, it was omitted from Table 3 of the same paper. It is listed as J175850.9–290106 in Alard et al. (2000), with $\log P = 2.158$: (144 d, uncertain). Its excess appears to begin at least by the K -band. It is very red at mid-IR wavelengths, with $K - [7] = 1.61$ and $[7] - [15] = 1.98$ (Omont et al. 2001).

In addition, during the preparation of this diagram, two ISOGAL/MACHO stars (J175903.0–290137 and JJ175916.9–290225) that appeared to be about a magnitude fainter than the others in K_S were investigated and found to have been dropped from the final ISOGAL Catalogue (Omont et al., 2001), i.e., they are MACHO stars not identified with reliable mid-infrared sources.

5 COLOUR-COLOUR DIAGRAMS

In what follows we include some solar neighbourhood giants for comparison purposes. These have been derived from the spectrophotometric atlases of LW and Pickles (1998). Their colours have been calculated assuming the ESO and DENIS photometric response functions. Recourse to this ‘synthetic’ photometry, based on spectrophotometry, is necessary because no data that combine the I band with JHK_S exist outside the DENIS work.

Fig 6 presents the $(I - J)_0$ vs $(J - K_S)_0$ diagram. There is a continuous well-defined sequence from left to right. The LW and Pickles (1998) stars cover the giants from medium to late spectral types. By comparison with the colours of the latter, it is apparent that the clumped DENIS objects are predominantly of K- and early M-type, with smaller numbers of earlier and later types. The ISOGAL/MACHO stars without dust show a rapid increase in $(I - J)_0$ with $(J - K_S)_0$ colour as the I -band strength decreases due to increasing TiO and VO absorption at lower temperatures. Finally, the most extreme colours are shown by the stars with dust excesses that are also the most luminous. The sequence shows much greater scatter about a given point in $(I - K_S)_0$ and $(I - J)_0$ than in $(J - K_S)_0$.

Fig 7 shows the $(J - H)_0, (H - K_S)_0$ diagram. Again a clear sequence is seen from the LW and Pickles (1998) stars through the great mass of 2MASS objects, to the ISOGAL/MACHO stars. The average colours of Miras in Sgr I from Glass et al. (1995), computed for various period groups and shifted to the right by 0.07 mag, to allow for the difference in the K filters, are also shown as a solid line.

In general, the $J - H$ and $H - K$ colours, which are sensitive to metallicity (see comparison of LMC and Sgr I Miras in Glass et al. 1995) and atmospheric extension (Bessell et al. 1989), of the SRVs and Miras of the Baade’s Window population agree closely with the solar neighbourhood sample.

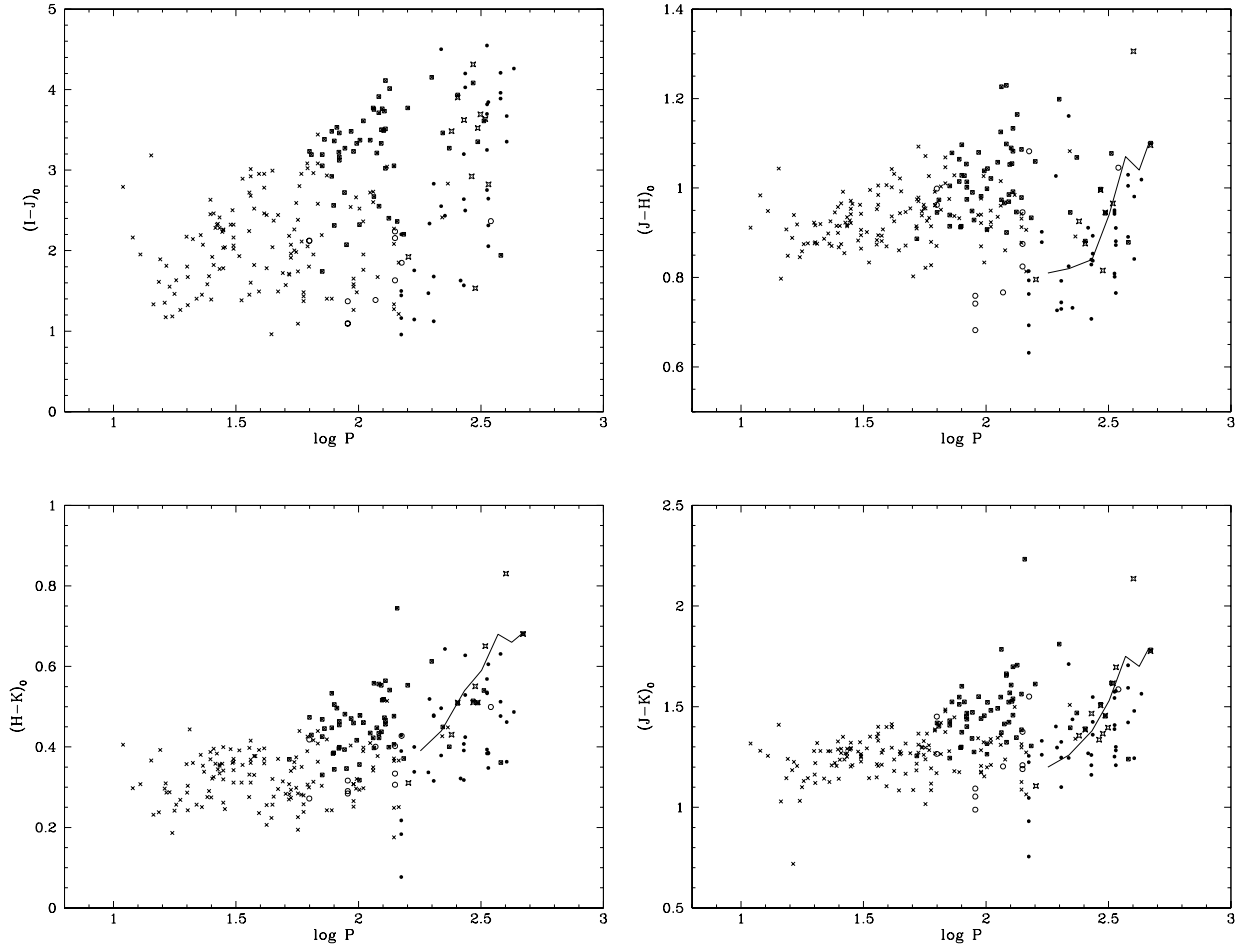


Figure 8. Colour-period diagrams for ISOGAL/MACHO stars. (a) (Top left) $(I - J)_0$ vs $\log P$ from DENIS. The crosses represent SRVs without appreciable mass-loss and solid squares those with mass-loss. The starred symbols represent Mira variables from ISOGAL/MACHO. Also included are LW SRVs (open circles) and Miras (filled circles), calculated for the DENIS filters. (b) (Top right) $(J - H)_0$ vs $\log P$ from 2MASS for ISOGAL/MACHO Bulge SRVs. The averaged colours of Sgr I Miras for various period groups from Glass et al. (1995) are also shown. Other symbols as in (a), above. The displacement to lower $(J - H)$ of the Miras is a well-known phenomenon but its dependence on pulsation period is shown here for the first time. (c) (Bottom left) $(H - K)_0$ vs $\log P$ from 2MASS. Information as in (b), above. (d) (Bottom right) $(J - K)_0$ vs $\log P$ from 2MASS. Information as in (b), above.

6 COLOUR-PERIOD DIAGRAMS

The periods of the SRVs are by their very nature not very well-defined. The techniques for determining them from the MACHO data and their limitations have been described by Alard et al. (2001). Essentially, the periods given here are those that were dominant during the years of the MACHO observations. In some cases, other (usually nearby) periods had nearly equal Fourier amplitudes.

Fig 8 shows the colour-period plots for the available samples.

One should recollect that appreciable mass-loss is only seen for those stars that have periods in excess of 70d (Alard et al. 2001), but a longer period does not guarantee that it will occur. This is also true of field SRVs, as found from CO observations (Kerschbaum Olofsson & Hron 1996). The colours of Miras can vary by 0.1 mag or more around a cycle. Note that an individual variable star from LW may be represented by more than one point in these diagrams

since their observations were often made at more than one phase.

6.1 $I - J$ vs $\log P$

In all colours it is apparent that the colours of the SRVs increase on the average with period. However, it is noticeable that the scatter in I at a given period is 3–4 mags whereas in the other colours it is much less (up to 0.7). Alvarez et al. (2000) show that there is a close relationship (s.d. = 0.09 mag) of wide validity between $I - M_{\text{bol}}$ and $(I - J)$ colour for O-rich stars. The Miras do not show any clear colour-period relation.

6.2 $J - H$ vs $\log P$

Because of the poor overlap between the available 2MASS data and the NGC 6522 ISOGAL field, most of the stars in the diagrams involving the H -band are from Sgr I. It is

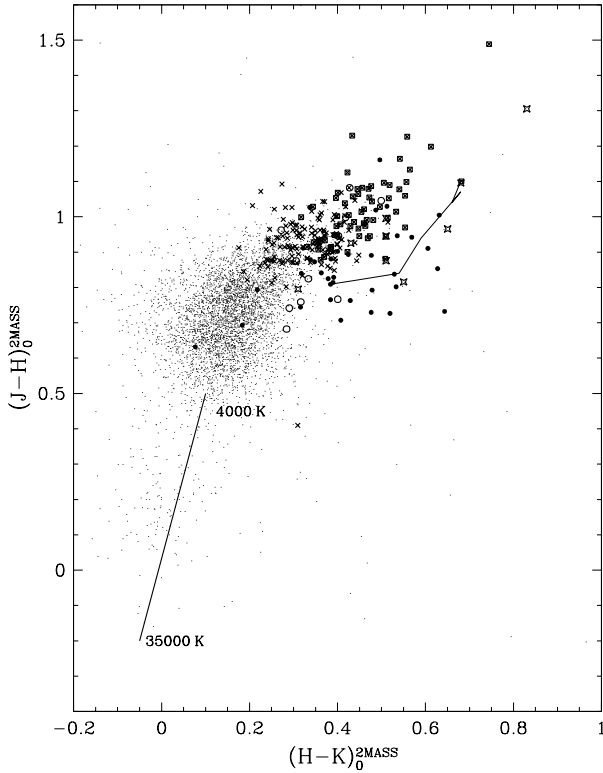


Figure 7. $(J-H)_0, (H-K)_0$ diagram from 2MASS. Crosses represent ISO GAL/MACHO SRVs with low mass-loss; squares represent those with high. Small points represent the remainder of stars in Sgr I. The straight line shows the location of earlier-type giants from Pickles (1998). The bent line is the location of the average colours of Mira variables in Sgr I, taken from Glass et al. (1995) and shifted by 0.07 mag in $H-K$ to allow for the difference between the SAAO and 2MASS K filters. Open circles are synthetic colours of SRVs and solid circles are Miras derived from the LW spectrophotometry. The three bluest (in $H-K$) Mira points are amongst those representing the 150d hot Mira S Car.

expected that the observed $(J-H)$ colours will not differ significantly between the 2MASS and ESO or SAAO systems.

The semiregulars show a moderate increase in $(J-H)_0$ colour with period. They overlap, particularly at the longer-period end, the field SRVs (e.g., Kerschbaum & Hron 1994, not shown in the figures in order to avoid confusion). Our knowledge of the statistics of short-period field SRVs is limited at present by their small amplitudes and the consequent difficulty of detecting them by traditional methods. Only recently have systematic studies become possible using photometry from the Hipparcos satellite (Bedding & Zijlstra 1998; Koen & Laney, 2000).

That the Miras are displaced from the region of SRVs in the $J-H, H-K$ diagram has been known for many years (see e.g. Feast et al, 1982, and references therein). The LW atlas shows definitively that stars which exhibit strong H_2O absorption bands during their pulsation cycles have large amplitudes. Now that this effect can be displayed on a $J-H, \log P$ diagram (fig. 8b), the displacement caused by the water-vapour absorption bands is seen to be quite dramatic

at periods of about 150–200 days. In this connection, it is also interesting to note that the spectra of Bulge Miras can be matched very closely by non-Mira spectra differing only by the absence of H_2O features (LW).

The observed $J-H$ colours from Glass et al. (1995) are slightly redder on average than the points derived from the LW spectrophotometry of field Miras, though similar to the colours obtained by Kerschbaum (unpublished) and others for field Miras. This difference may reflect the difficulty of allowing for the terrestrial atmospheric water vapour absorption in deriving the synthetic photometry.

We also comment that the LW points representing T Cen, classed as a SRV (open circles) with period 90d ($\log P = 1.95$), are unusually low in this and the other colour-period diagrams. Its visual amplitude of 3.5 mag is excessive for a SRV, suggesting that it is a Mira variable of unusually short period.

6.3 $H-K_S$ vs $\log P$

The $(H-K_S)_0$ colours of the SRVs increase with period in much the same way as the $(J-H)_0$. It is more noticeable in this diagram than in the $(J-H)$ vs $\log P$ that the SRVs with $[7]-[15]$ excesses are redder than those without, at a given period. The LW points for field SRVs are in agreement with the SRVs of similar period with low mass-loss.

The Miras form a well-defined sequence which, however, starts below the average $(H-K_S)_0$ of the SRVs at the same period (~ 180 d). The Sgr I relation appears to straddle the LW field Miras satisfactorily, though the scatter of the latter is rather large.

6.4 $J-K_S$ vs $\log P$

The $(J-K_S)_0$ index, like the others, increases steadily with period for the SRVs, especially those with strong mass-loss from $[7]-[15]$ photometry. The redder colours of the mass-losing objects are even more obvious.

7 K_S VS $\log P$ DIAGRAM

A version of this diagram, based on transformed $7\mu\text{m}$ mags, was presented by Alard et al. (2001). It is given here with K_S mags directly from 2MASS. The conclusions of Alard et al. remain unchanged.

Absolute K magnitudes of SRVs with periods are available for only a few other samples. They include nearby objects with parallaxes from the Hipparcos Catalogue (Bedding & Zijlstra, 1998) and those in the Large Magellanic Cloud (Wood, 2000) with periods also derived from MACHO. Whitelock (1986) showed that SRVs in low-metallicity galactic globular clusters exhibit a P-L sequence that falls about 0.8 mag below that of Bedding & Zijlstra.

In the Large Magellanic Cloud the Miras, the SRVs and the small-amplitude SRVs seem to form distinct parallel sequences C, B, A etc (see fig. 9) which have been identified by Wood (2000) as pulsators in the fundamental, first and the next two higher overtones respectively. The present data do not show such clearly separated sequences except perhaps between the Miras and the others. The effect may be

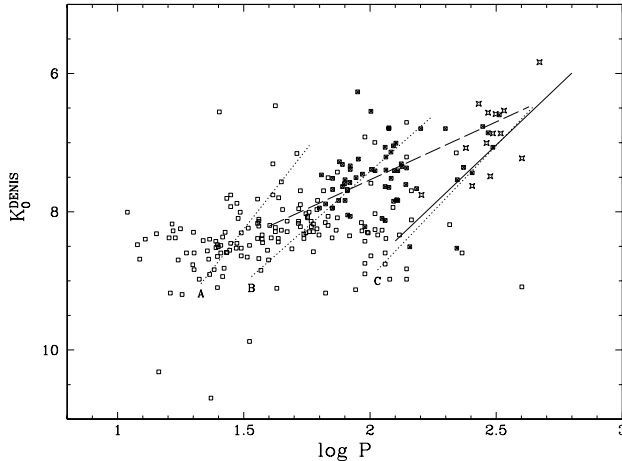


Figure 9. $K_{S,0}$, $\log P$ diagram for both Baade's Window fields. The squares represent ISOGAL/MACHO sources; the filled ones have high mass-loss. The solid line is the locus of Miras in Sgr I from Glass et al. (1995), offset by 0.05 mag downwards in K to allow for the difference in photometric systems. Miras in the sample are indicated by the starred symbols. The dashed line is the relationship suggested for local SRVs by Bedding & Zijlstra (1998). The dotted lines labelled A,B and C are eye fits to LMC sequences by Wood (2000). We have taken 3.8 mags as the difference in distance moduli between the LMC and the Bulge, as determined from the Mira $P - L$ relation (Glass et al 1995), and we have assumed an LMC distance modulus of 18.55.

blurred in the Galactic Centre relative to the Large Magellanic Cloud by the depth in the line of sight of the Bulge. For example, the scatter of the *averaged K* mags of Miras about the P-L relation is 0.35 mag for the latter as compared to 0.13 for the LMC (Glass et al. 1987).

Included in the diagram is a P-L sequence for the Hipparcos (nearby) SRVs from Bedding and Zijlstra (1998). Similar lines, which cross the loci of the various pulsation modes, were predicted by Vassiliadis & Wood (1993) as evolutionary sequences, their absolute luminosity depending on initial mass and metallicity. The position of the line suggests that there is little difference between the Bulge and local samples. The spectra of Mira variables in the Bulge can also be matched well by local Miras (LW).

8 CONCLUSIONS

In the Baade's Windows K_S , $J - K$ diagram the most luminous stars are the Miras and SRVs. The SRVs with significant mass-loss are generally more luminous than those without.

The average $I - J$, $J - H$, $H - K$ and $J - K$ colours of the SRVs increase with period but the effect is much less pronounced if the mass-losing stars are omitted. The scatter in the colours of SRVs is greatest in $I - J$. In all the colours considered here, scatter increases with period.

The average $J - H$ colours of the shorter-period Bulge Miras (~ 200 d) are much bluer than the average of the SRVs with similar periods. A similar but less conspicuous discontinuity occurs in the $H - K$ and $J - K$ colours. This effect is attributed to the onset of H_2O absorption, which affects

H and K more than J . In each of $J - H$, $H - K$ and $J - K$, the average Mira colours show steeper rates of increase with period than the SRVs.

The colours of solar neighbourhood SRVs and Miras, derived for the DENIS and 2MASS systems from the LM spectrophotometry, agree with those of the Bulge. In addition, the locations in the K , $\log P$ diagram of the SRVs, which should be sensitive to any differences in initial mass and metallicity, are in good agreement.

9 ACKNOWLEDGMENTS

We thank A. Lançon for her help in calculating the synthetic near-IR colours of stars from the spectrophotometry of LW and A. Omont for his helpful comments. We also thank F. Kerschbaum for access to unpublished photometry.

MS thanks SAAO and ISG thanks the IAP for their hospitality during visits financed through the CNRS (France)/NRF (South Africa) agreement.

MS is supported by the Fonds zur Förderung der wissenschaftlichen Forschung (FWF), Austria, under the project number J1971-PHY.

The DENIS project is supported, in France by the Institut National des Sciences de l'Univers, the Education Ministry and the Centre National de la Recherche Scientifique, in Germany by the State of Baden-Württemberg, in Spain by the DGICYT, in Italy by the Consiglio Nazionale delle Ricerche, in Austria by the Fonds zur Förderung der wissenschaftlichen Forschung und Bundesministerium für Wissenschaft und Forschung

This publication makes use of data products from the Two Micron All Sky Survey, which is a joint product of the University of Massachusetts and the Infrared Processing and Analysis Center/California Institute of Technology, funded by the National Aeronautics and Space Administration and the National Science Foundation.

REFERENCES

- Alard C. et al., 2001, ApJ, 552, 289
- Alvarez R., Lançon A., Plez B., Wood P.R., 2000, A&A, 353, 322
- Bedding T.R., Zijlstra A.A., 1998, ApJ, 506, L47
- Bessell M.S., Brett J.M., Scholz M., Wood P.R., 1989, A&A, 213, 209
- Blanco V.M., 1986, AJ, 91, 290
- Blanco V.M., McCarthy M.F., Blanco B.M., 1984, AJ, 89, 636
- Bouchet P., Schmider F.X., Manfroid J., 1991 A&AS, 91, 409
- Epchtein N., 1998, In The Impact of Large Scale Near-IR Sky Surveys, eds N. Epchtein, Kluwer, p. 3
- Feast M.W., Robertson B.S.C., Catchpole R.M., Lloyd Evans T., Glass I.S., Carter B.S., 1982, MNRAS, 201 439
- Fouqué P. et al., 2000, A&AS, 141, 313
- Frogel J.A., Whitford A.E., 1987, ApJ, 320, 199 (see also 1990, ApJ 357, 453, concerning revised spectral types)(FW)
- Glass I.S., 1993, In Precision Photometry, Proc. Conf to Honour AWJ Cousins in his 90th Year, Sth Afr Astr Obs, 1993, p. 119
- Glass I.S., 1986, MNRAS, 221, 879
- Glass I.S., 1999, Handbook of Infrared Astronomy, Cambridge University Press.
- Glass I.S. et al., 1999, MNRAS, 308, 127
- Glass I.S., Catchpole R.M., Feast M.W., Whitelock P.A., Reid I.N., 1987, in Late Stages of Stellar Evolution, ed. S. Kwok & S.R. Pottasch (Dordrecht: Reidel)

- Glass I.S., Whitelock P.A., Catchpole R.M., Feast M.W., 1995, MNRAS, 273, 383
 Kerschbaum F., Hron J., 1994, A&AS, 106, 397
 Kerschbaum F., Olofsson H., Hron J., 1996, A&A, 311, 273
 Koen C., Laney C.D., 2000, MNRAS, 311, 636
 Lançon A., Wood P.R., 2000, A&AS, 146, 217 (LW)
 Lloyd Evans, T., 1976, MNRAS, 174, 169
 Omont A., et al., 1999, A&A, 348, 755
 Omont A., et al., 2001, A&A, in preparation
 Persson S.E., Murphy D.C., Krzeminski W., Roth M., Rieke M.J., 1998, ApJ, 116, 247
 Pickles, A.J., 1998, PASP, 110, 863
 Skrutskie M.F., 1998, In The Impact of Large Scale Near-IR Sky Surveys, eds N. Epchtein, Kluwer, p. 11
 Vassiliadis E. & Wood P.R., 1993, ApJ, 413, 641
 Whitelock P.A., 1986, MNRAS, 219, 528
 Wood P.R., 2000, Proc Astr Soc Austr, 17, 18